ARTICLE

pubs.acs.org/Biomac

Diels−Alder Click Cross-Linked Hyaluronic Acid Hydrogels for Tissue Engineering

Chelsea M. Nimmo,[†,‡] Shawn C. Owen,[†,§,∥] and Molly S. Shoichet*[,†,‡,§,∥]

[†]The Donnelly Centre for Cellular and Biomolecular Research, [‡]Department of Chemistry, [§]Department of Chemical Engineering and Applied Chemistry, and [∥]Institute of Biomaterials and Biomedical Engineering, University of Toronto, Toronto, Ontario, Canada

Supporting Information

ABSTRACT: Hyaluronic acid (HA) is a naturally occurring polymer that holds considerable promise for tissue engineering applications. Current cross-linking chemistries often require a coupling agent, catalyst, or photoinitiator, which may be cytotoxic, or involve a multistep synthesis of functionalized-HA, increasing the complexity of the system. With the goal of designing a simpler one-step, aqueous-based cross-linking system, we synthesized HA hydrogels via Diels−Alder "click" chemistry. Furan-modified HA derivatives were synthesized and cross-linked via dimaleimide poly(ethylene glycol). By controlling the furan to maleimide molar ratio, both the mechanical and degradation properties of the resulting Diels−Alder cross-linked hydrogels can be tuned. Rheological and degradation studies demonstrate that the Diels−Alder click reaction is a suitable cross-linking method for HA. These HA cross-linked hydrogels were shown to be cytocompatible and may represent a promising material for soft tissue engineering.

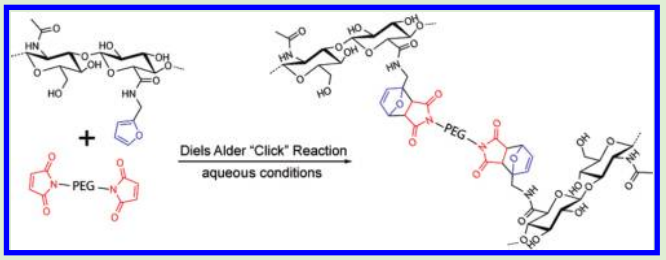

1. INTRODUCTION

Hyaluronic acid (HA) is a naturally occurring nonsulfated glycosaminoglycan found ubiquitously in the extracellular matrix (ECM) with reported roles in embryonic development, tissue organization, wound healing, and angiogenesis.[1] HA is also biocompatible and biodegradable and elicits low levels of immune response, offering considerable promise for tissue engineering and wound-healing.[2] Over the past decade, a wide variety of HA-based hydrogels has been engineered, demonstrating dural repair,[3] sustained cell expansion,[4,5] facilitated cartilage repair,[6] oriented bone regeneration,[7] and directed neural progenitor cell differentiation,[8] among others. These scaffolds can be manipulated to mimic aspects of the extracellular microenvironment. For example, inclusion of cell-adhesive peptides (RGD)[9] and ECM proteins (collagen)[10] within HA scaffolds can enhance cellular attachment and spreading. Other polymer molecules, such as poly(ethylene glycol) (PEG),[6,9] have also been included in HA hydrogels to vary the mechanical properties and pore size of the scaffolds.

Native HA is water-soluble and exhibits a fast degradation profile and clearance within the body.[1,11] Therefore, HA must be covalently cross-linked to provide a mechanically robust hydrogel. Cross-linking typically involves chemical modification of HA by targeting either the hydroxyl or carboxylic acid functionalities of the sugar moieties. For example, HA has been modified with mono- and polyvalent hydrazides, which in turn react with PEG-dialdehydes to form hydrogels.[12] This methodology has been extended with Huisgen click chemistry by cross-linking HA-azide and HA-alkyne derivates under copper catalysis.[13] HA hydrogels have also been synthesized using photochemistry with methacrylate-fuctionalized HA and photo-cross-linkers (Irgacure 2959 or eosin Y).[4,14] Therefore, a coupling agent, catalyst, or photoinitiator is often required for cross-linking, introducing potentially cytotoxic small molecules and hence lowering the biocompatibility of the material. These hydrogels must be extensively washed to remove catalysts or unreacted coupling agents before the addition of cells. This is a laborious process that can lead to undesired hydrogel degradation.

Thiolated-HA can be cross-linked without additives via disulfide bond formation upon oxidation; however, synthesis of thiolated-HA is a time-consuming, multistep process that can negatively impact the native structure of HA by decreasing the molecular weight.[15] Moreover, the inclusion of thiols in the HA backbone may complicate cross-linking reactions in the presence of cysteine-containing peptides or proteins. These may react with HA-thiols, resulting in disulfide bond formation, thereby affecting their structure and function. Furthermore, thiol-disulfide oxidoreduction of cell surface proteins plays a role in regulating critical cellular functions such as adhesion and proliferation,[16] and thus a blank hydrogel canvas without thiols allows more control over cellular behavior.

An ideal methodology to create HA hydrogels is composed of aqueous-based orthogonal cross-linking chemistry that is free of additives and is achieved in a simple one-step reaction. To this

Received: December 1, 2010
Revised: January 19, 2011
Published: February 11, 2011

Scheme 1. Synthesis of Furan-Modified HA Derivative (HA-Furan)

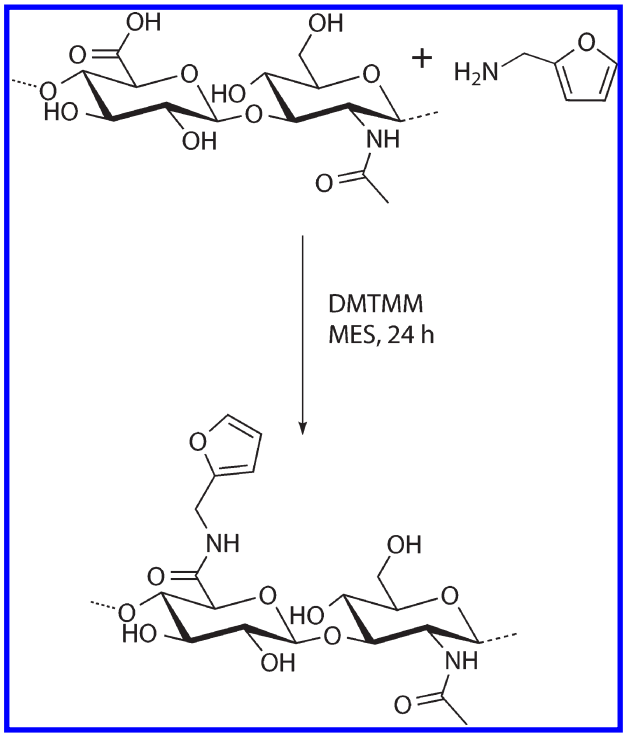

end, we report a new synthesis of HA hydrogels based on Diels–Alder chemistry. The Diels–Alder reaction is a highly selective [4 + 2] cycloaddition between a diene and a dienophile that is greatly accelerated in water.[17,18] Furthermore, the Diels–Alder reaction is a "click"-type reaction[19] between orthogonal molecules that is free from side reactions and byproduct. We have previously exploited this chemistry for conjugation of antibodies to nanoparticles for targeted drug delivery,[20] and others have used it to create synthetic polymeric hydrogels.[21,22] Here we demonstrate the applicability of Diels–Alder click chemistry to synthesize cross-linked HA hydrogels. In this simple, one-step cross-linking strategy, stable hydrogels are formed without the use of an initiator, catalyst, or coupling agent from an HA derivative. Furan-modified HA (diene) was first synthesized using 4-(4,6-dimethoxy-1,3,5-triazin-2-yl)-4-methylmorpholinium chloride (DMTMM) and then used to form HA hydrogels cross-linked via dimaleimide poly(ethylene glycol) (dienophile) linkers in aqueous solution. The synthesis of these Diels–Alder HA hydrogels is described herein and characterized in terms of their mechanical properties, degradation, and cellular interactions.

2. MATERIALS AND METHODS

2.1. Materials. Dried sodium hyaluronate (HA) (2.34×10^5 amu), was purchased from Lifecore Biomedical (Chaska, MN). Bis-maleimido-poly(ethylene glycol) ($(MI)_2$PEG) (3.0×10^4 amu) was purchased from RAPP Polymere GmbH (Tülbingen, Germany). Furfurylamine was supplied by Acros Organics (Geel, Belgium). 4-(4,6-Dimethoxy-1,3,5-triazin-2-yl)-4-methylmorpholinium chloride (DMTMM), D_2O, and KBr were purchased from Aldrich Chemistry (St. Louis, MO). 2-(*N*-Morpholino)-ethanesulfonic acid (MES) buffer and hyaluronidase (Type IV–S, lyophilized powder, 2140 units/mg) were purchased from Sigma Life Sciences (St. Louis, MO). Dulbecco's phosphate buffered saline (DPBS) and RPMI-1640 cell culture media were purchased from Multicell Technologies (Woonsocket, RI). Dialysis membranes were purchased from Spectrum Laboratories (Rancho Dominguez, CA). Human adenocarcinoma cells (MDA-MB-231) were purchased from ATCC (Manassas, VA) catalog number HTB-26.

2.2. Synthesis and Characterization. *2.2.1. Synthesis and Characterization of HA-Furan (Scheme 1).* Furan-modified HA (HA-furan) derivatives were synthesized by dissolving HA (0.40 g, 1.02 mmol) in 40 mL of MES buffer (100 mM, pH 5.5) to which DMTMM was added in 4 (1.13 g, 4.08 mmol), 2 (0.56 g, 2.04 mmol), or 1 (0.28 g, 1.02 mmol) molar ratio (relative to the −COOH groups in HA) and stirred for 10 min. Furfurylamine was then added dropwise in a 2 (188.8 μL, 2.04 mmol), 1 (94.4 μL, 1.02 mmol), or 0.5 (47.2 μL, 0.51 mmol) molar ratio (relative to the −COOH groups in HA). The reaction was conducted at room temperature for 24 h and then dialyzed against distilled water for 3 days (M_w cutoff 12 000−14 000 Da). Water was removed by lyophilization to obtain HA-furan derivatives as a white powder. The degree of substitution (DS) was determined from ^{1}H NMR spectra by comparing the ratio of the areas under the proton peaks at 6.26, 6.46, and 7.65 ppm (furan protons) to the peak at 1.9 ppm (*N*-acetyl glucosamine protons of HA). ^{1}H NMR spectra were recorded in D_2O on a Varian Mercury-400 MHz NMR spectrometer (Palo Alto, CA).

2.2.2. Synthesis of HA-PEG Hydrogels (Scheme 2). HA-PEG hydrogels were synthesized by reacting HA-furan with $(MI)_2$PEG cross-linker separately in MES buffer (100 mM, pH 5.5). The concentration of HA-furan was held constant at 1.5% w/v, whereas the concentration of $(MI)_2$PEG was varied to examine differences in hydrogel properties as a function of the molar ratio of furans (HA-furan) to the molar ratio of maleimides ($(MI)_2$PEG). For example, 15 mg of HA-furan (DS 57.5%, 19.3 μmol of furan) was dissolved in 1 mL of MES buffer. $(MI)_2$PEG was dissolved in MES buffer at different concentrations: either 14.48 (9.65 μmol of maleimide, furan/MI 1:0.5), 28.95 (19.3 μmol of maleimide, Furan/MI 1:1), or 57.92 mg (38.6 μmol of maleimide, furan/MI 1:2) in 375 μL of MES buffer. HA-furan and $(MI)_2$PEG solutions were combined and vortexed to ensure thorough mixing. Samples were allowed to gel at room temperature. The final concentration of HA-furan in the hydrogels was always 1.1% w/v, whereas the total polymer concentration (HA + PEG) within the hydrogels was either 2.1 (1Furan/0.5MI), 3.2 (1Furan/1MI), or 5.3% w/v (1Furan/2MI). Herein, HA hydrogels are referenced according to the furan to maleimide molar ratios as 1Furan/0.5MI, 1Furan/1MI, or 1Furan/2MI.

2.2.3. FTIR Spectroscopy of HA-PEG Hydrogels. Fourier transform infrared (FTIR) spectra were recorded for HA, HA-furan, $(MI)_2$PEG, and dry cross-linked HA-PEG hydrogels to characterize the −C═C− in the Diels–Alder adduct, indicating chemical cross-linking. Spectra were recorded with a Spectrum 1000 FT-IR spectrometer (Waltham, MA), collecting 32 scans in the 400−4000 cm^{-1} range with a resolution of 2 cm^{-1}.

2.2.4. Rheological Characterization of HA-PEG Hydrogels. The viscoelastic mechanical properties of the HA-PEG hydrogels were measured with an AR-1000 rheometer fitted with a 60 mm, 2° acrylic cone using parallel plate geometry (TA Instruments, New Castle, DE). Upon casting the hydrogels (1 mL), the upper plate was immediately lowered to a gap size of 20 μm. Hydrogels were allowed to cure overnight at 37 °C using an integrated Peltier plate before testing. A frequency sweep was conducted from 0.1 to 630 rad/s at 0.1% strain to determine the shear elastic modulus (G') of hydrogels following a stress sweep test to confirm that the frequency and strain were within the linear viscoelastic region. Sample evaporation was minimized using a solvent trap.

2.2.5. Equilibrium Swelling of HA-PEG Hydrogels. To examine swelling properties, cross-linked HA-PEG hydrogel samples (100 μL) were synthesized in preweighed vials according to the above procedure

Scheme 2. Schematic Representation of the Formation of the Diels-Alder HA-PEG Hydrogels by Crosslinking HA-Furan with $(MI)_2$PEG

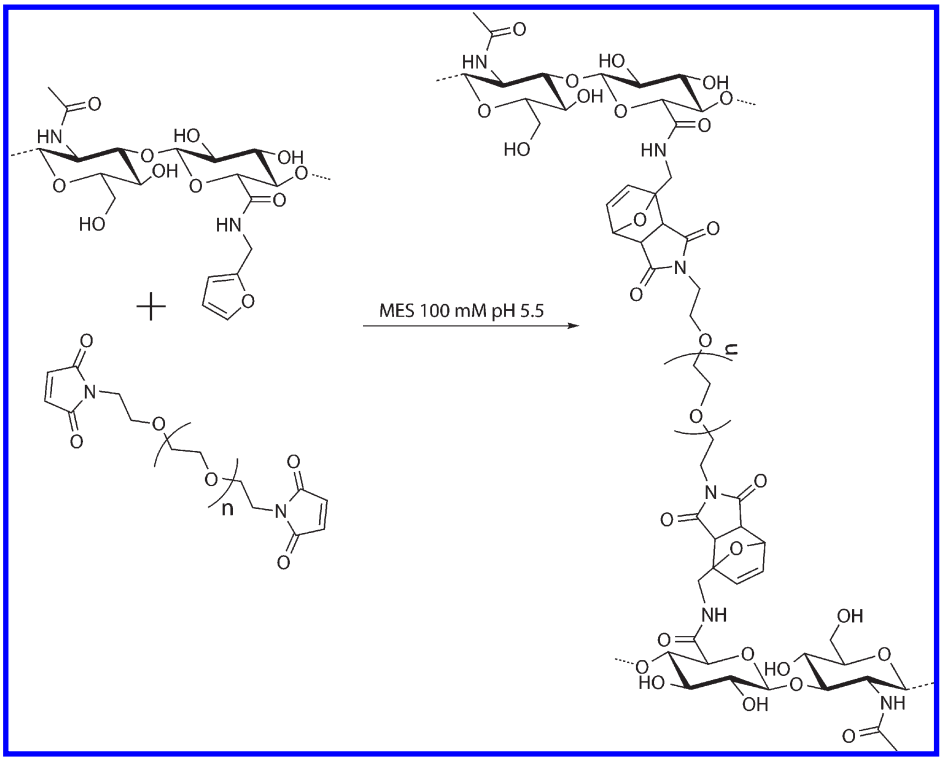

and accurately weighed (M_0). Samples (n = 15) were then incubated in 1 mL of DPBS buffer (100 mM, pH 7.4) at 37 °C. At select time points, the swelling ratio was determined by measuring the mass (M_t), following removal of buffer, and gently drying the hydrogel surface with a tissue. Hydrogels were then replenished with fresh buffer. From these data, swelling ratios (M_t/M_0) were calculated, and the equilibrium swelling ratio was recorded when the mass of the gels no longer increased.

2.2.6. Degradation Assay. To determine the stability of the HA-PEG hydrogels, we synthesized samples (100 μL) in preweighed vials according to the above procedure and allowed them to swell in DPBS (100 mM, pH 7.4) for 24 h at 37 °C, after which the mass of the samples was measured (M_s). Degradation experiments were performed using 50 U mL^{-1} hyaluronidase in DPBS at 37 °C. At selected time points, the supernatant was removed, hydrogels were weighed (M_t), and percent of hydrogel mass remaining relative to the original swollen mass was calculated (M_t/M_s). Fresh buffer containing hyaluronidase was replaced in each sample at each time point. Degradation profiles were also recorded for hydrogels incubated in DPBS at 37 °C with no enzyme present as a negative control.

2.2.7. Cell Culture and Viability. Human epithelial cells (MDA-MB-231) were maintained (fewer than six passages) in plastic culture flasks in RPMI 1640 growth medium with 10% fetal bovine serum (FBS), 10 UI/mL penicillin, and 10 μg/mL streptomycin. HA-PEG hydrogels were prepared as described, and 350 μL samples were pipetted in sterile four-well chamber slides (Lab-Tek). Hydrogels were left overnight to ensure complete gelation and then washed with culture media prior to cell plating. Cells were plated on top of each gel at a density of 3.0×10^4 cells per well in medium and maintained in a tissue culture incubator (37 °C, 5% CO_2, 95% humidified). Medium was exchanged every two to three days for 14 days, after which images were captured with a Zeiss Axiovert S100 (Carl Zeiss MicroImaging GmBH, Germany) inverted microscope equipped with an X-Cite 120 fluorescence illumination system (EXFO, Ontario, Canada) and a CoolSNAP HQ digital camera (Photometrics, Tucson, AZ) using Image-Pro Plus software (Media Cybernetics, Silver Spring, MD). To test cell viability, 14 day cultures were treated using the LIVE/DEAD cell viability assay (Invitrogen, Carlsbrad, CA) as per the manufacturer's instructions. Three representative images were captured for each gel, and the number of live and dead cells was recorded (n = 6 gels).

2.3. Statistical Analysis. All statistical analyses were performed using GraphPad Prism version 5.00 for Windows (GraphPad Software, San Diego, CA, www.graphpad.com). Differences among groups were assessed by one-way ANOVA with Bonferroni post hoc correction to identify statistical differences among three or more treatments. A p value of $\leq$0.05 was set as the criteria for statistical significance. Graphs are annotated where p values are represented as * $\leq$ 0.05, ** $\leq$ 0.01, or *** $\leq$ 0.001. All data are presented as mean $\pm$ standard deviation.

3. RESULTS AND DISCUSSION

3.1. Synthesis and Characterization of HA-Furan. HA-furan derivates were prepared in a simple, one-step reaction by coupling furfurylamine to HA carboxylates using 4-(4,6-dimethoxy-1,3,5-triazin-2-yl)-4-methylmorpholinium chloride (DMTMM) reagent (Scheme 1). DMTMM has been recognized as a highly efficient activator of polysaccharide carboxyl groups in aqueous conditions, superior to traditional carbodiimide coupling.[23] In a reaction with 1-[3-(dimethylamino) propyl]-3-ethylcarbodiimide hydrochloride (EDCI), the yield of immobilization of furfurylamine on HA was much lower than that using DMTMM (Supporting Information). By varying the molar ratios of HA/furfurylamine/DMTMM, variable degrees of substitution, defined as the number of furans per HA disaccharide repeat, were obtained. Molar ratios of 1:2:4, 1:1:2, and 1:0.5:1 yielded HA-furan with 75 $\pm$ 8% (n = 4),

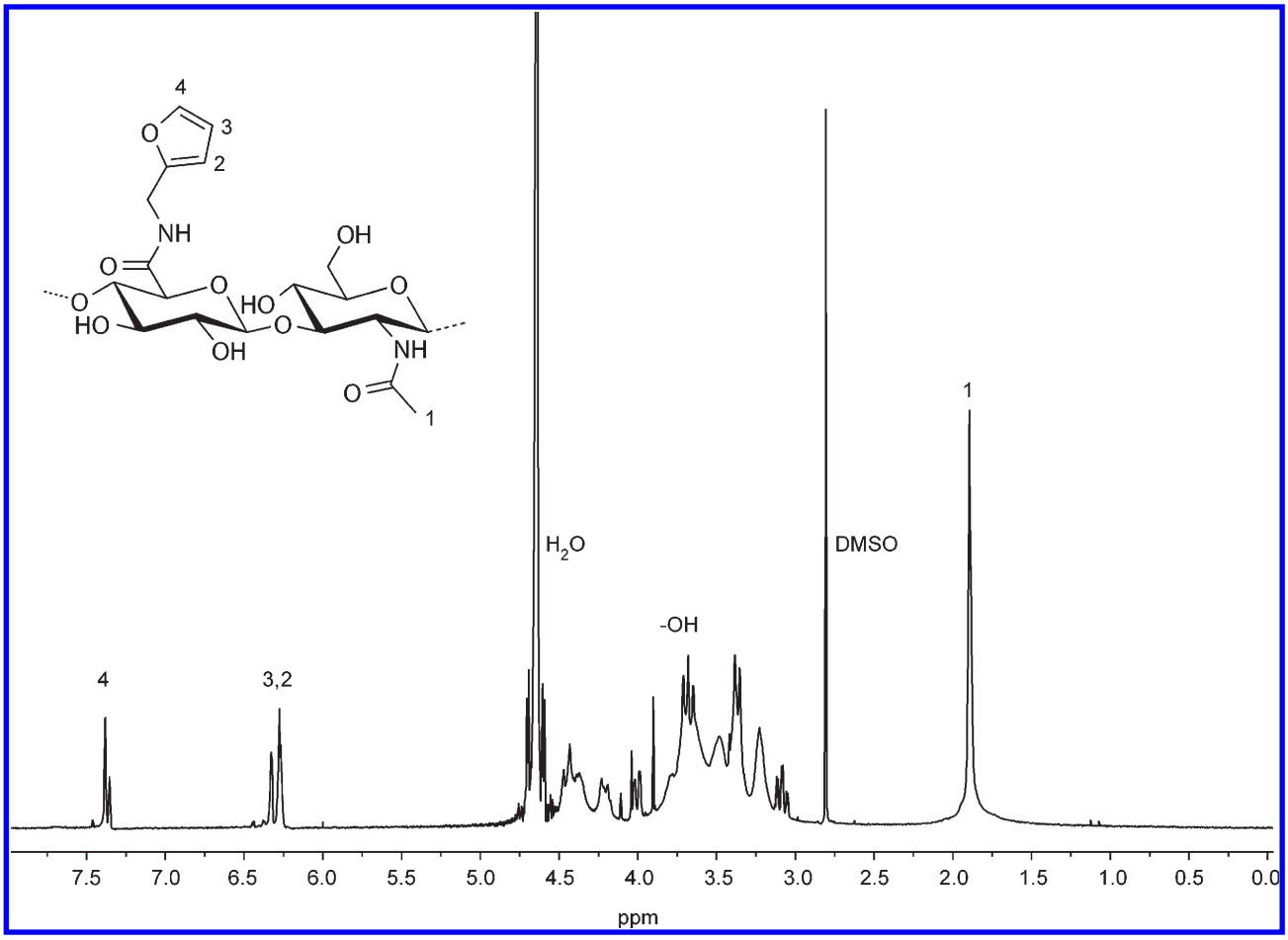

Figure 1. ^{1}H NMR spectra in D_2O (400 MHz) of HA-furan (DS = 54%). Degree of substitution was determined by comparing the integrated areas under the proton peaks at 6.26, 6.46, and 7.65 ppm (furan protons), indicated by 2, 3, and 4 to that of the peak at 1.9 ppm (*N*-acetyl glucosamine of HA), indicated by 1.

61 ± 7% (n = 4), and 49 ± 6% (n = 9) degrees of substitution, respectively (Supporting Information). The structure and DS was confirmed by ^{1}H NMR (Figure 1). Resonances at 6.26, 6.46, and 7.65 ppm verified the presence of furan protons, and their integrated ratios were compared with that of the *N*-acetyl glucosamine proton peak of native HA, appearing at 1.9 ppm. For the remaining studies, HA-furan with a DS of 49% was employed because lower substituted HA hydrogels have been shown to display higher cellular bioactivity.[24]

3.2. FTIR Characterization of HA-PEG Hydrogels. HA-PEG hydrogels were synthesized by mixing solutions of HA-furan and $(MI)_2$PEG cross-linker in MES buffer (pH 5.5) (Scheme 2). Figure 2 displays FTIR spectra of HA, HA-furan, $(MI)_2$PEG, and the cross-linked HA-PEG hydrogel. Conjugation of furfurylamine to the carboxylic acid on HA results in a shift of the C═O stretch on HA at 1617 to 1653 cm^{-1}, characteristic of amide bond formation. Analysis of HA-furan and $(MI)_2$PEG spectra reveals C═C peaks at 1455 and 1466 cm^{-1} corresponding to the furan on HA-furan and the maleimide on $(MI)_2$PEG, respectively. Alkene bending is also quite apparent within the $(MI)_2$PEG spectrum with a sharp signal at 695 cm^{-1}, representing the C═C of the maleimide. The hydrogel spectrum shows decreased absorption of these C═C signals and increased absorption at 1459 cm^{-1} (C═C in adduct), indicating the consumption of individual furan and maleimide groups and the formation of a maleimide-furan adduct during the Diels−Alder reaction.

3.3. Rheological Characterization of HA-PEG Hydrogels. The mechanical properties of HA-PEG hydrogels were characterized by oscillatory rheology studies using parallel plate geometry at 37 °C. The aim of the rheological measurements was to characterize the G' value, the shear elastic modulus, for each HA-PEG hydrogel upon completion of the cross-linking reaction. In all cases, G' was independent of frequency, indicating that hydrogels were cross-linked prior to recording measurements (Supporting Information). Hydrogels were analyzed corresponding to their furan:maleimide (Furan/MI) ratio, that is, their cross-linker concentration. In all experiments, the molar furan concentration was held constant while the molar maleimide concentration was varied. Cross-linker concentration was altered to distribute molar ratios of either 1Furan/1MI, 1Furan/0.5MI, or 1Furan/2MI within hydrogels. As shown in Figure 3a, the elastic modulus of the hydrogels increased with higher cross-linker concentrations. There was significant difference between all hydrogel formulations ($p < 0.001$) where increased maleimide concentrations resulted in higher cross-link density via the formation of additional Diels−Alder adducts. Accordingly, 1Furan/0.5MI hydrogels were the weakest with a G' value of 275 ± 54 Pa, whereas 1Furan/2MI hydrogels were the strongest with a G' value of 679 ± 62 Pa. The elastic modulus of 1Furan/1MI

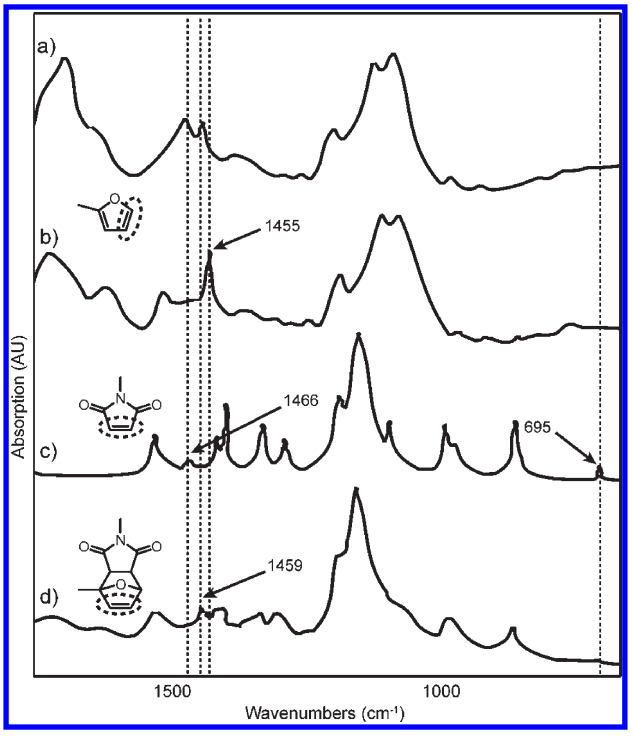

Figure 2. FTIR spectra of (a) HA, (b) HA-furan showing the C=C absorbance from furan at 1455 cm^{-1}, (c) $(MI)_2$PEG showing the C=C absorbance from maleimide at 1466 cm^{-1} and =C−H bending at 695 cm^{-1}, and (d) cross-linked HA-PEG showing a decrease in both the 695, 1455, and 1466 cm^{-1} peaks and the appearance of a new peak at 1459 cm^{-1} corresponding to the C=C bond in the Diels−Alder adduct.

hydrogels was 557 ± 37 Pa, approximately double the strength of 1Furan/0.5MI hydrogels. Because G' increased from 1Furan/1MI to 1Furan/2MI, it is apparent that the reaction between the furan and maleimide does not proceed to 100% conversion. However, the G' doubling effect between 1Furan/0.5MI and 1Furan/1MI was not maintained between 1Furan/1MI and 1Furan/2MI, indicating that G' reaches a plateau with an increased cross-linker concentration. These results confirm that Diels−Alder click chemistry is efficient in the formation HA hydrogels.

In tissue engineering, it is important to consider the mechanical properties of the tissue of interest.[25] The shear moduli of the HA-PEG hydrogels are similar to those of brain and nerve tissues (100−1000 Pa),[26] thus making them compelling scaffolds for neural tissue engineering. By varying other parameters, such as the DS, molecular weight, or concentration of HA-furan, the shear moduli may be further manipulated to mimic those of connective tissue, liver, and the mammary fat pad, among others. For example, the shear elastic moduli of liver, fat, relaxed muscle, and breast gland tissue ranges from 1000−10 000 Pa.[27−29] These values could be achieved by using a higher molecular weight HA or a higher HA weight concentration.[26]

3.4. Equilibrium Swelling. The swelling behavior of HA-PEG hydrogels was monitored by mass after incubation in DPBS at 37 °C. Swelling ratios reached a plateau after 24 h (Supporting Information), and reported values are taken from this time point (Table 1). Whereas the data are significantly different ($p < 0.001$, $n = 15$), the values are effectively quite similar. 1Furan/0.5MI hydrogels swelled the most. This was expected because the 1Furan/0.5MI gels have the lowest cross-link density of the

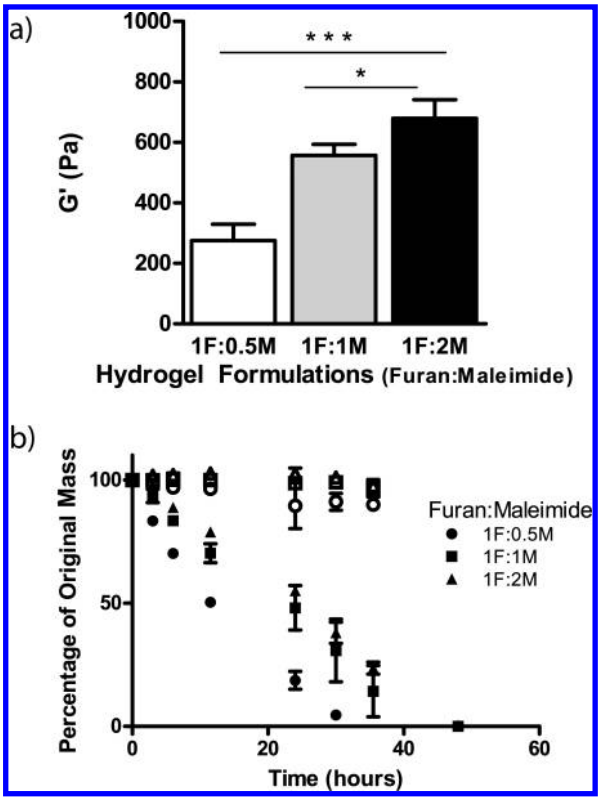

Figure 3. (a) Rheological characterization of HA-PEG hydrogels. Increasing the concentration of cross-linker results in a stiffer gel. The difference between gels with a 1Furan/1MI ratio and a 1Furan/2MI ratio is not as great as that between 1Furan/0.5MI and 1Furan/1MI, suggesting efficient cross-linking (average elastic modulus ± standard deviation, $n = 4$). (b) In vitro HA-PEG hydrogel degradation. Solid shapes: samples incubated in PBS with 50 U mL^{-1} of hyaluronidase. Open shapes: samples incubated in PBS (control) (average percentage of original weight ± standard deviation $n = 3$).

Table 1. Equilibrium Swelling Data (Average ± Standard Deviation, $n = 15$)

hydrogel formulation	equilibrium swelling ratio	$(MI)_2$PEG concentration (% wt/v)
1Furan/0.5MI	1.48 ± 0.03	0.95
1Furan/1MI	1.39 ± 0.04	1.89
1Furan/2MI	1.44 ± 0.04	3.78

three formulations. This is consistent with the degree of equilibrium swelling of a polymeric hydrogel being inversely proportional to its elastic modulus.[30] Surprisingly, 1Furan/2MI hydrogels had a similar equilibrium swelling ratio to the 1Furan/0.5MI samples, and both were greater than that of 1Furan/1MI gels. Because 1Furan/2MI hydrogels displayed the greatest shear elastic modulus, the higher equilibrium swelling ratio cannot be accounted for by the rubber elasticity theory. The equilibrium swelling ratio of the 1Furan/0.5MI hydrogels has fewer cross-links and thus swells more, whereas the 1Furan/2MI imbibes more water because of a greater concentration of PEG cross-linker.

3.5. Degradation Assay. To monitor in vitro degradation of HA-PEG hydrogels, samples were incubated in DPBS with 50 U mL^{-1} of hyaluronidase versus PBS alone at 37 °C, and their

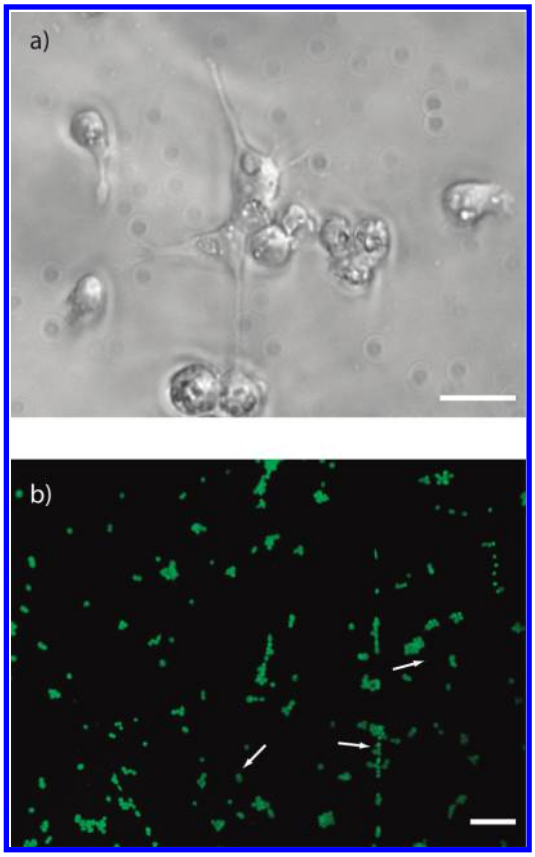

Figure 4. (a) Representative image of MDA-MB-231 cells grown on HA-PEG hydrogels for 14 days showing morphology characteristics of cell attachment (40× magnification, scale bar = 20 μm). (b) Live/dead assay demonstrating the high level of cell survival (>98%). Live cells (green) and dead cells (red: indicated by arrows) are seen on hydrogels after 14 days in culture (10× magnification, scale bar = 60 μm).

masses were recorded over 52 h. Samples incubated in PBS (controls) showed no significant mass loss after 52 h, whereas samples incubated in hyaluronidase were completely degraded in this time frame. Degradation rates were calculated from the linear slope of the percentage of original mass versus time (Figure 3b). Degradation rates directly correlated with cross-linker concentration, with 1Furan/0.5MI hydrogels degrading the fastest at 3.40 ± 0.19%/h and 1Furan/2MI hydrogels degrading the slowest at 2.06 ± 0.04%/h. 1Furan/1MI hydrogels displayed an intermediate degradation profile at 2.23 ± 0.06%/h. The degradation rate of 1Furan/0.5MI hydrogels was significantly greater compared with 1Furan/1MI and 1Furan/2MI hydrogels; however, there was no significant difference ($p > 0.05$) between 1Furan/1MI and 1Furan/2MI hydrogels. These results suggest that the difference in the number of cross-links within 1Furan/1MI and 1Furan/2MI hydrogels did not impact degradation appreciably, suggesting a sufficient cross-linking efficiency for Diels−Alder HA hydrogels. This conclusion is consistent with that derived from the rheological data.

Importantly, enzymatic recognition was retained with the furan-modification of HA, suggesting that HA-PEG hydrogels are suitable for applications in tissue engineering. In vivo, predicted degradation rates for HA-PEG hydrogels would be much slower because physiological hyaluronidase levels are much lower than that used in this study. Whereas degradation was only monitored with respect to cross-linker concentration, varying the HA weight percent would expand the degradation profile.[24]

3.6. Cell Attachment and Viability. The morphology and viability of endothelial cells was assessed after 14 days of culture in vitro. MDA-MB-231 cells were selected because they express CD44, the receptor for HA, allowing for cell interaction and potential adhesion to the HA-PEG hydrogels used in this study.[31] Cells plated on the hydrogels remained rounded for the first 24 h, after which the majority of cells began to adopt a flattened morphology, suggesting cell attachment, as shown in Figure 4a. Cells continued to spread and remained attached to hydrogels for the duration of the experiment.

Cell viability was evaluated using a live/dead assay that stains live cells green (calcein AM) and dead cells red (ethidium homodimer). HA-PEG hydrogels showed a high level of cell survival (>98%), as seen in Figure 4b, demonstrating the cytocompatibility of the hydrogels. It is important to note that a significant number of cells initially seeded onto hydrogels did not adhere to the gels and were removed during media exchange. Nevertheless, several cells attached and proliferated, suggesting a CD44 interaction with HA.

4. CONCLUSIONS

Diels−Alder chemistry is an effective cross-linking method to prepare hydrogels from furan-modified HA and dimaleimide-functionalized PEG. Synthesis of the scaffold backbone, HA-furan, was achieved in a single step. Synthesis of the hydrogel required neither additional cross-linking agents nor catalysts, resulting in a clean, one-step synthetic procedure. The HA-PEG hydrogels had an elastic modulus similar to that of central nervous system tissue and demonstrated minimal swelling and complete degradation. Together with their cell-interactive properties, these HA-PEG hydrogels are likely suitable for applications in tissue engineering and regenerative medicine.

■ ASSOCIATED CONTENT

Supporting Information. Controllable DS of HA-furan synthesis by varying the ratio of HA/Furfurylamine/DMTMM or with the coupling agent EDCI, representative frequency sweeps of 1Furan/0.5MI, 1Furan/1MI, and 1F/2MI, and equilibrium swelling with respect to time plot of HA-furan hydrogels. This material is available free of charge via the Internet at http://pubs.acs.org.

■ AUTHOR INFORMATION

Corresponding Author
*E-mail: molly.shoichet@utoronto.ca.

■ ACKNOWLEDGMENT

We are grateful for funding from NSERC (MSS) and the CIHR Training Program in Regenerative Medicine (CMN).

■ REFERENCES

(1) Allison, D. D.; Grande-Allen, K. J. *Tissue Eng.* **2006**, *12*, 2131–2140.
(2) Termeer, C.; Sleeman, J. P.; Simon, J. C. *Trends Immunol.* **2003**, *24*, 112–114.
(3) Gupta, D.; Tator, C. H.; Shoichet, M. S. *Biomaterials* **2006**, *27*, 2370–2379.

(4) Baier Leach, J.; Bivens, K. A.; Patrick, C. W., Jr.; Schmidt, C. E. *Biotechnol. Bioeng.* **2003**, *82*, 578–589.
(5) Burdick, J. A.; Chung, C.; Jia, X.; Randolph, M. A.; Langer, R. *Biomacromolecules* **2005**, *6*, 386–391.
(6) Jin, R.; Teixeira, L. S. M.; Krouwels, A.; Dijkstra, P. J.; van Blitterswijk, C. A.; Karperien, M.; Feijen, J. *Acta Biomater.* **2010**, *6*, 1968–1977.
(7) Patterson, J.; Siew, R.; Herring, S. W.; Lin, A. S. P.; Guldberg, R.; Stayton, P. S. *Biomaterials* **2010**, *31*, 6772–6781.
(8) Seidlits, S. K.; Khaing, Z. Z.; Petersen, R. R.; Nickels, J. D.; Vanscoy, J. E.; Shear, J. B.; Schmidt, C. E. *Biomaterials* **2010**, *31*, 3930–3940.
(9) Shu, X. Z.; Ghosh, K.; Liu, Y. C.; Palumbo, F. S.; Luo, Y.; Clark, R. A.; Prestwich, G. D. *J. Biomed. Mater. Res., Part A* **2004**, *68A*, 365–375.
(10) Park, S. N.; Park, J. C.; Kim, H. O.; Song, M. J.; Suh, H. *Biomaterials* **2002**, *23*, 1205–1212.
(11) Kang, C. E.; Poon, P. C.; Tator, C. H.; Shoichet, M. S. *Tissue Eng., Part A* **2009**, *15*, 595–604.
(12) Luo, Y.; Kirker, K. R.; Prestwich, G. D. *J. Controlled Release* **2000**, *69*, 169–184.
(13) Crescenzi, V.; Cornelio, L.; Di Meo, C.; Nardecchia, S.; Lamanna, R. *Biomacromolecules* **2007**, *8*, 1844–1850.
(14) Park, Y. D.; Tirelli, N.; Hubbell, J. A. *Biomaterials* **2003**, *24*, 893–900.
(15) Shu, X. Z.; Liu, Y. C.; Luo, Y.; Roberts, M. C.; Prestwich, G. D. *Biomacromolecules* **2002**, *3*, 1304–1311.
(16) Skalska, J.; Brookes, P. S.; Nadtochiy, S. M.; Hilchey, S. P.; Jordan, C. T.; Guzman, M. L.; Maggirwar, S. B.; Briehl, M. M.; Bernstein, S. H. *PLoS ONE* **2009**, *4*, e8115.
(17) Otto, S.; Engberts, J. B. *Org. Biomol. Chem.* **2003**, *1*, 2809–2820.
(18) Rideout, D. C.; Breslow, R. *J. Am. Chem. Soc.* **1980**, *102*, 7816–7817.
(19) Kolb, H. C.; Finn, M. G.; Sharpless, K. B. *Angew. Chem., Int. Ed.* **2001**, *40*, 2004–2021.
(20) Shi, M.; Wosnick, J. H.; Ho, K.; Keating, A.; Shoichet, M. S. *Angew. Chem., Int. Ed.* **2007**, *46*, 6126–6131.
(21) Wei, H. L.; Yang, Z.; Chen, Y.; Chu, H. J.; Zhu, J.; Li, Z. C. *Eur. Polym. J.* **2010**, *46*, 1032–1039.
(22) Kosif, I.; Park, E. J.; Sanyal, R.; Sanyal, A. *Macromolecules* **2010**, *43*, 4140–4148.
(23) Farkas, P.; Bystrický, S. *Carbohydr. Polym.* **2007**, *68*, 187–190.
(24) Eng, D.; Caplan, M.; Preul, M.; Panitch, A. *Acta Biomater.* **2010**, *6*, 2407–2414.
(25) Shoichet, M. S. *Macromolecules* **2010**, *43*, 581–591.
(26) Vanderhooft, J. L.; Mann, B. K.; Prestwich, G. D. *Biomacromolecules* **2007**, *8*, 2883–9.
(27) Chen, E. J.; Novakofski, J.; Jenkins, W. K.; Obrien, W. D. *IEEE Trans. Ultrason. Ferroelectr. Freq. Control* **1996**, *43*, 191–194.
(28) O'Hagan, J. J.; Samani, A. *Phys. Med. Biol.* **2009**, *54*, 2557–2569.
(29) Discher, D. E.; Mooney, D. J.; Zandstra, P. W. *Science* **2009**, *324*, 1673–1677.
(30) Anseth, K. S.; Bowman, C. N.; BrannonPeppas, L. *Biomaterials* **1996**, *17*, 1647–1657.
(31) Sheridan, C.; Kishimoto, H.; Fuchs, R. K.; Mehrotra, S.; Bhat-Nakshatri, P.; Turner, C. H.; Goulet, R., Jr.; Badve, S.; Nakshatri, H. *Breast Cancer Res.* **2006**, *8*, R59.